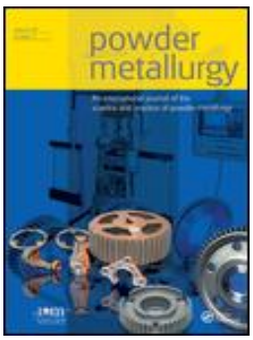

Powder Metallurgy

ISSN: 0032-5899 (Print) 1743-2901 (Online) Journal homepage: http://www.tandfonline.com/loi/ypom20

SPS-assisted Synthesis of SIC_p reinforced high entropy alloys: reactivity of SIC and effects of pre-mechanical alloying and post-annealing treatment

E. Colombini, M. Lassinantti Gualtieri, R. Rosa, F. Tarterini, M. Zadra, A. Casagrande & P. Veronesi

To cite this article: E. Colombini, M. Lassinantti Gualtieri, R. Rosa, F. Tarterini, M. Zadra, A. Casagrande & P. Veronesi (2017): SPS-assisted Synthesis of SIC_p reinforced high entropy alloys: reactivity of SIC and effects of pre-mechanical alloying and post-annealing treatment, Powder Metallurgy, DOI: 10.1080/00325899.2017.1393162

To link to this article: http://dx.doi.org/10.1080/00325899.2017.1393162

Published online: 03 Nov 2017.

POWDER METALLURGY, 2017
https://doi.org/10.1080/00325899.2017.1393162

The Institute of Materials, Minerals and Mining

Taylor & Francis
Taylor & Francis Group

SPS-assisted Synthesis of SiC_p reinforced high entropy alloys: reactivity of SiC and effects of pre-mechanical alloying and post-annealing treatment

E. Colombini [a], M. Lassinantti Gualtieri [a], R. Rosa[a], F. Tarterini[b], M. Zadra[c], A. Casagrande[b] and P. Veronesi[a]

[a]Department of Engineering 'Enzo Ferrari', University of Modena and Reggio Emilia, Modena, Italy; [b]Department of Industrial Engineering, Alma Mater Studiorum-University of Bologna, Bologna, Italy; [c]K4Sint, Pergine Valsugana, Italy

ABSTRACT

In this work a traditional high entropy alloy (FeCoNiCrAl) was reinforced by uniformly distributed reactive silicon carbide (SiC) particles by a powder metallurgy synthetic route, using as precursors simply mixed powders or mechanically prealloyed ones. The reactive sintering produced a single isomorphic BCC structure. The sample microstructure resulted equiassic, more homogenous in samples based on prealloyed powders. The instability of SiC in the presence of metal precursors resulted in the formation of more stable carbides and silicides, as well as in carbon diffusion in the high entropy alloy matrix and partially unreacted SiC particles. The formation of these newly formed fine precipitates, as well as the presence of residual SiC were useful to increase the hardness of the alloy.

ARTICLE HISTORY
Received 2 May 2017
Revised 28 September 2017
Accepted 11 October 2017

KEYWORDS
Spark plasma sintering; reinforcement; high entropy alloys; powder metallurgy; SIC; hardness

Introduction

Traditional alloys are typically composed of one or two main elements, but a new class of metallic materials composed of at least five major components [1–3] with nearly equiatomic concentration have attracted much attention across the world, due to their unique properties [4], such as high hardness, strength, [5] wear resistance [6] corrosion resistance [7] and excellent mechanical properties both at high and low temperature [8–10]. Conventionally, simple solid solution structures, such as FCC or BCC, are formed due to the high entropy effect which balances the enthalpy of mixing [11]. Hence, this new class of alloys has been called high entropy alloys (HEAs). According to the literature [7,12–14], the most employed processing routes for synthesising HEAs are: from the liquid state (e.g. melting and casting) [7,13–19], from the solid state (powder metallurgy,[17,20–22]), from the gas state (sputtering techniques, [7,14]) and via electrochemical processes [23]. Among the solid state routes, the most used ones are mechanical alloying [17] and spark plasma sintering (SPS) [21]. Nevertheless a new synthetic method has recently been explored by the present authors [24–27], using high frequency electromagnetic fields in the microwave range which enables to overcome the limits of current liquid state processes (defects formation, e.g. voids, dendritic structures) and solid state ones (time demanding, i.e. long synthesis due to slow diffusion processes) [24,28]. Electromagnetic field assisted preparation of HEAs (microwave, SPS) could benefit from the presence of a non-conductive or semi-conductive secondary phase, leading to the possibility of processing much larger samples, due to the increase of electromagnetic field penetration depth, and its higher efficiency [29]. In case of ceramic particles dispersed in a metallic precursors mixture, the differentiated heating of the phases is expected, due to differences in their electric, magnetic and dielectric properties. This could lead to the generation of peculiar temperature profiles during electromagnetic field exposure, which has already been exploited in the past for the manufacturing of composites using microwave heating [30].

The use of HEAs as matrixes for the generation of new composite materials with high toughness and hardness, accompanied by high wear and oxidation resistance at high temperature, constitutes a potentially interesting field of application for engineering structures, like engines and turbines. In this framework, HEAs were recently used as matrices in WC and Ti(C,N)-based cermets [31] or hosting 10 vol.-% silicon carbide (SiC) [32], to improve mechanical properties.

Metal matrix composites (MMCs) generally contain reinforcing ceramic particles, such as SiC, alumina (Al_2O_3), boron carbide (B_4C) and graphite (C), having high strength, high elastic modulus, wear and fatigue resistance are used as reinforcement to fabricate particulate composites [33,34]. However, from a thermodynamic point of view, SiC is relatively unstable in most metal matrixes if compared to oxides (Al_2O_3) and nitrides (Si_3N_4) [35,36]. Nevertheless, it is currently used in some MMCs thanks to the silica protective layer formed on the SiC surface in oxidising atmosphere [37]. In fact, this thin layer prevents

CONTACT E. Colombini elena.colombini@unimore.it Department of Engineering 'Enzo Ferrari', University of Modena and Reggio Emilia, Via Pietro Vivarelli 10, 41125 Modena, Italy

further oxidation at high temperature and increases the apparent stability and efficiency of SiC as reinforcement. However, in case of exposure to high temperature in an inert or slightly oxidative atmosphere, the thermodynamic instability of SiC becomes dominant in presence of transition metals [38,39].

According to literature [38,39], SiC particles inserted in a traditional HEA containing, for instance, Co, Fe, Ni or Cr, should react to form silicides and carbides starting from 800°C, with possible further liberation of Si or C which can enter the HEA to form substitutional or interstitial solid solutions.

Nevertheless, the sluggish diffusion [11,40], which is typical of many HEAs, ensures that some SiC can withstand the exposure to such metals at high temperature for a limited time period. Hence, SiC can be considered as a possible candidate as reactive reinforcement in HEAs, offering multiple strengthening mechanisms dictated by the formation of solid solutions, of silicides and carbides and by the residual presence of unreacted SiC. This has been partially demonstrated by some of the authors [26], who have investigated the effect of Si-modification on HEAs, demonstrating its role in increasing hardness and deflecting cracks. Among the HEA systems, FeCoCrNiCu and FeCoCrNiAl are the most studied ones [13,20]. In this work, the FeCoNiCrAl HEA was chosen as matrix as it contains elements which are good carbide and silicide formers.

The aim of this paper is to evaluate the feasibility of preparing HEAs matrix composites (FeCoNiCrAl reinforced by 10 wt-% SiC) starting from PM technology using mechanically prealloyed powders or mixed powders to investigate the effect of adding reactive ceramic particles as reinforcement of HEAs. The poor stability of SiC is expected to lead to the formation of more stable silicides and carbides. Hence, silicon and carbon are available for entering the solid solution of the HEA, thus modifying its microstructure and mechanical properties. Furthermore, if processing parameters are controlled so that an enough rapid synthesis is performed, residual partially reacted SiC can act as reinforcement, with possible formation of adhesive and continuous interfaces between matrix and reinforcement. The strong joints between metal and ceramic phases can be readily fabricated by nucleation and growth of reinforcement carbides inside the metal matrix [32,38]

Materials and methods

The elemental powders (Sigma Aldrich) that were used as reactants to prepare FeCoCrNiAl + 10 wt-% SiC are shown in Table 1.

Two different routes to prepare the precursor powder mixture were used:

- mechanical mixing by high energy milling for 40 minutes (activation)
- pre-alloying by high energy milling for 35 hours. This long milling time was chosen as literature data indicate that at least 15 hours are required to achieve mechanical alloying [25,40].

Table 1. Composition of the metal powders used (BCC = body centred cubic; FCC = face centred cubic; HCP = Hexagonal close-packed arrangement).

Element	Purity (%)	Particle size (μm)	Cell
Fe	97.00	<44	BCC
Co	99.80	<2	HCP
Ni	99.70	<5	FCC
Cr	99.00	<44	BCC
Al	99.00	<75	FCC
SiC	97.50	<40	HCP

Both mixing and mechanical alloying were carried out using a Planetary Ball Mill PM 100 by Retsch GmbH, at 250 rev min^{-1} in an argon atmosphere, with steel balls, BPR 10:1 and cycles of 20 min milling followed by a 5 min break time to avoid overheating of the mixture.

The powders were then reactively sintered in a DR.SINTER® SPS1050 (Sumitomo Coal & Mining, now SPS Syntex, Inc., Tokyo, Japan) apparatus with graphite punches and dies. All samples had cylindrical geometry with a height of 5 mm and a diameter of 20 mm. SPS was performed at a nominal maximum temperature of 1000°C (measured with a thermocouple inserted into a blind hole in the die wall), with an uniaxial pressure of 60 MPa. The heating rate was 100°C/min up to 950°C and 50°C/min up to the set sintering temperature. The maximum temperature and pressure were held for 5 minutes, before allowing the furnace to cool down to room temperature.

All samples were subsequently annealed at 1200°C for 50 h in a tubular furnace, in a reactor containing titanium-shavings as getters, to reduce oxidative effects. The heat treatment was performed to improve samples homogeneity, leading to the possible formation of a single-phase (BCC solid solution in case of the investigated system).

The crystal structure was characterised by using an X-ray diffractometer (X'Pert PRO – PANAlytical) with Cu-Ka radiation and the microstructure was observed, after metallurgical preparation and etching by saturated $FeCl_3$ in C_2H_5OH-30%, with optical microscope Reichert-Jung. High-magnification micrographs and semi-quantitative chemical analyses were carried out using Scanning Electron Microscopy (SEM/ESEM – Quanta200 – FEI and SEM/FEG Nova NanoSEM 450 – FEI) in conjunction with energy dispersive spectrometry (EDS). Instrumented nano indentation (CSM Instruments) was used to perform depth-sensing nano-indentation tests. A 100 mN force with linear loading/unloading rate of 150 mN/min was applied for 15 seconds. The indentations were performed using a Berkovich tip and the elastic modulus and equivalent Vickers hardness were calculated

according to the Oliver and Pharr method [41]. Microhardness tests (Wolpert group 402 MVD instrument, Vickers, Wilson Wolpert Instruments, Aachen, Germany) were carried out as well, using 1 kg load.

Results

The use of SPS allowed to consolidate the powders in less than 30 minutes, including cooling.

To confirm the formation of HEAs following SPS, XRD analyses were carried out and the results are shown in Figure 1. As can be observed, independently of the precursors used (i.e. mixed or prealloyed powders) the formation of two solid solutions (BCC and FCC) is evident and can be ascribed to an incomplete interdiffusion of the metal species, given the extremely short synthesis time [28]. A more detailed discussion of these results combined with EDS analyses is presented later in this paper. However, despite the rapid reactive sintering, the SiC particles appear to have already reacted with the matrix. This is evidenced in Figure 2, which shows a BSE image of a SiC particle (black) embedded in the HEA matrix Figure 2(a), and the corresponding Si and Cr elemental map Figure 2(b). The infiltration of the HEA matrix (in purple) in the partially decomposed SiC as well as the Si outward diffusion (black dots) is evident (Figure 2 (b)). The interface interaction is evident also from the images shown in Figure 3, where the reactivity of SiC in the presence of mixed or prealloyed powders is compared. The microstructures of as-synthesised FeCoNiCrAl with 10 wt-% of SiC, before any annealing heat treatment, starting from mixed powders are shown on the left (Figure 3 (a–c)), while the microstructures in case of prealloyed powders are shown on the right (Figure 3 (b–d)). In both cases, the HEA embeds the partially decomposed SiC particles (darker particles in the low magnification micrographs in Figure 3(a) and Figure 3(b)), which in case of mixed powders present more rounded edges, indicating reactions with a transient liquid phase. The micrographs with higher magnification (Figure 3(c) and Figure 3(d)) show a single SiC particle infiltrated with the HEA. The area fraction occupied by the infiltrating alloy (light grey phase) is much higher in the case of mixed powders than in case of prealloyed powders. This could be noticed also macroscopically by monitoring the displacement of the piston in the SPS equipment as a function of temperature, as shown in Figure 3 (e–f). A significantly higher displacement occurs when using mixed powders. The displacement is given by two concurrent phenomena: at low temperatures, the prealloyed powders are already reinforced by solid solution formation and the high energy milling strain hardened the alloy; at higher temperature, when softening takes place and the first liquid phase is expected to appear, a much higher piston displacement is registered in case of mixed powders. This could be ascribed, for the same applied SPS cycle, to the formation of a larger quantity of liquid phase in case of mixed powders. This liquid phase formation could be ascribed to the exothermal contribution deriving from the reactions leading to the formation of the HEA, which, instead, had already been released in case of prealloying. Moreover, during SPS the SiC particles embedded in mixed powders are exposed to transition metals and their alloys, while they are exposed to an already formed

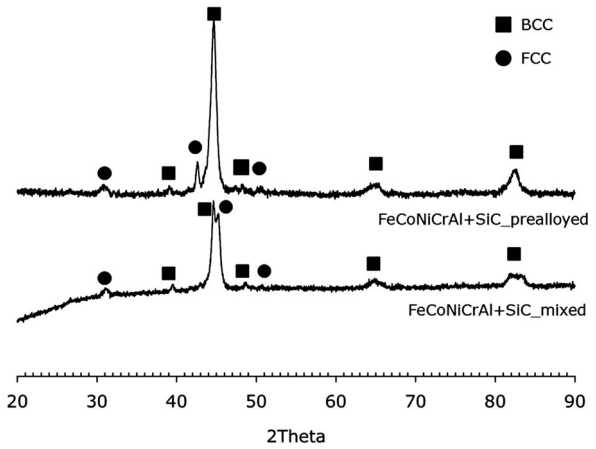

Figure 1. XRD pattern from powder to HEAs of FeCoNiCrAl after synthesis.

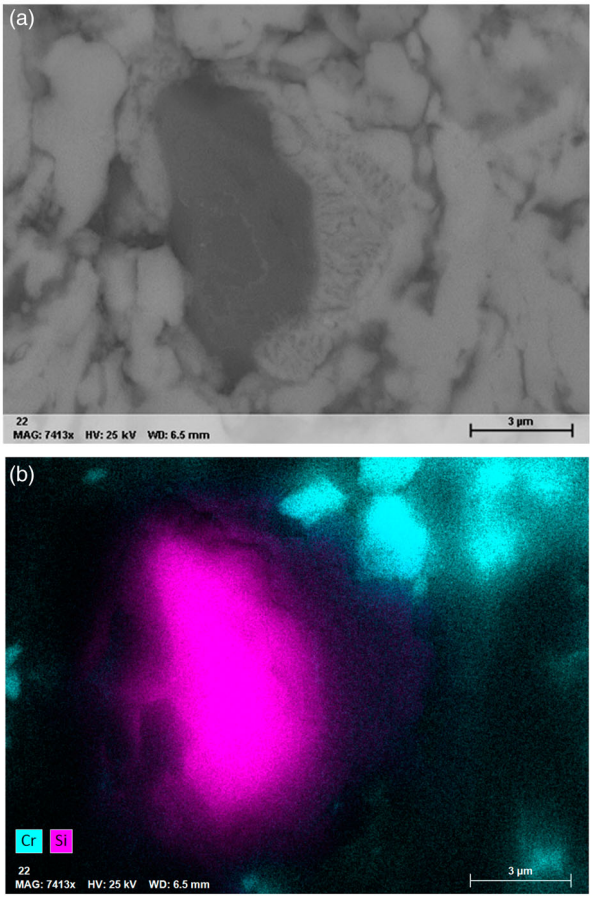

Figure 2. FeCoNiCrAl + SiC after SPS (a) SiC decomposition (b) distribution map of Si e Cr.

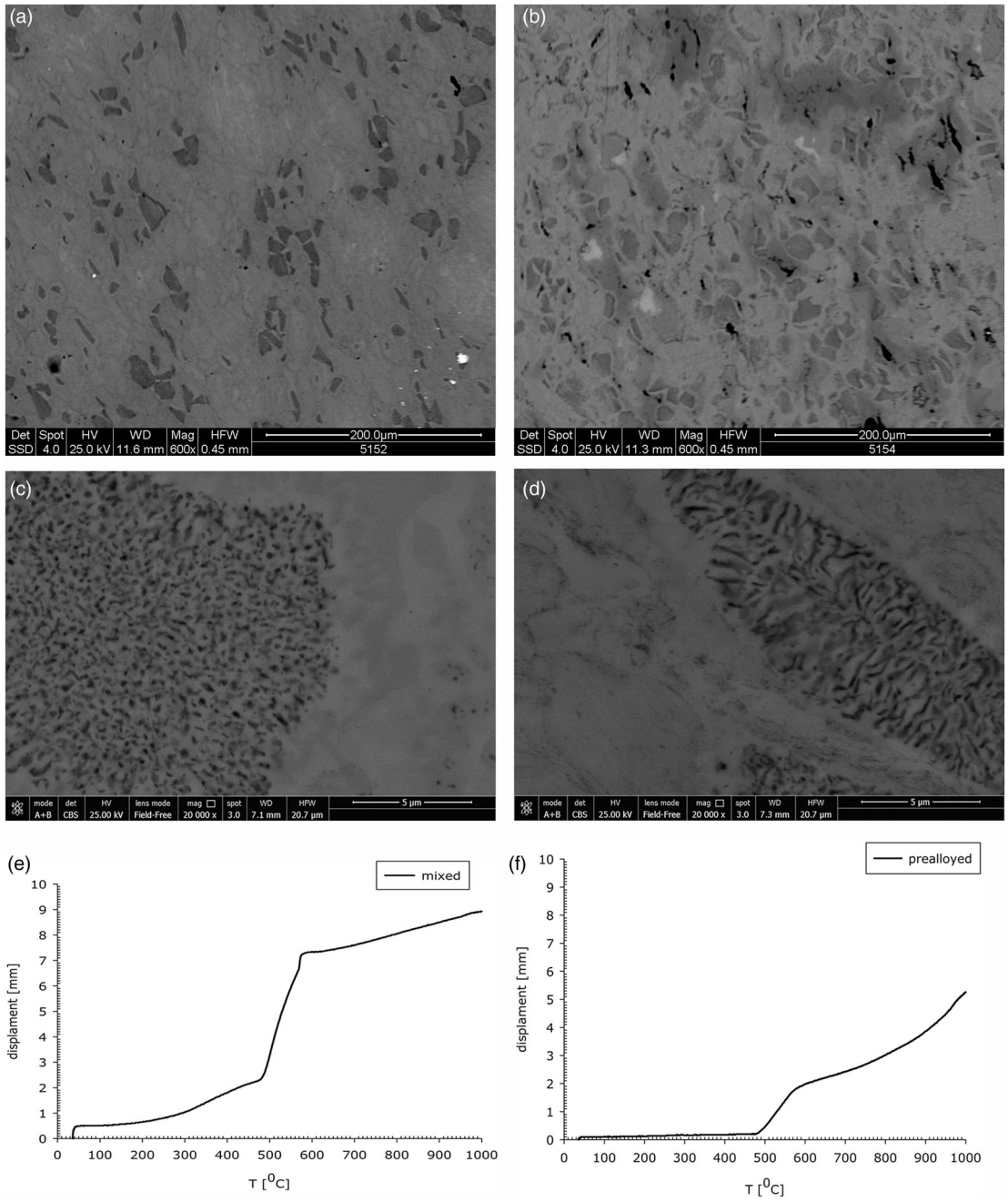

Figure 3. Microstructure of MPEAs after synthesis: FeCoNiCrAl + 10%SiC (a–c) mixed and (b–d) prealloyed after SPS, plot of displacement vs temperature during SPS synthesis of mixed (e) and prealloyed (f) powders.

HEA in case of prealloyed powders. This, as discussed later, has significant effects on the way SiC instability occurs at high temperature. Hence, the use of different powders has consequences on the SiC reactivity in the as-synthesised samples, but such differences are expected to be mitigated after prolonged annealing.

The diffraction patterns after the annealing heat treatment, which is expected to improve homogeneity, are shown in Figure 4. Only one phase (BCC) is present in both systems. This can be ascribed to the possible positive effect of Si (and Al) which promote the formation of a BCC structure [40].

The X-ray diffraction patterns after annealing also show the presence of Cr-carbides (Cr_7C_3) as labelled in Figure 4. Cr silicides are present as well. As expected, SiC is unstable in the presence of transition metals such as Co, Ni, Fe, Cr [38]. This instability, favoured by the long time exposure to 1000°C during annealing, results into the inclusion of Si in the HEA matrix, the fine precipitation of metal transition silicides and chromium carbides and possible diffusion of the excess carbon in the HEA matrix. The latter was investigated indirectly by nano-hardness measurements and shown later. The great negative free-energy formation of HEAs, the relatively low-temperature liquid formation through eutectic reactions may provide the driving force [41] to offer thermodynamic conditions which makes SiC unstable. Due to the SiC instability

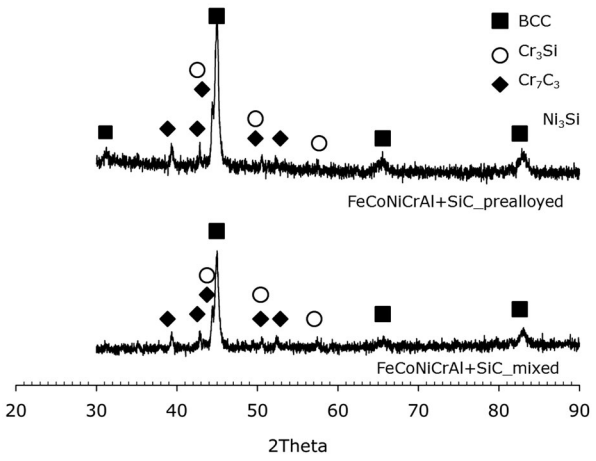

Figure 4. XRD pattern of HEAs synthesised after heat treatment.

[38], two types of SiC-Me reactions are possible [42]: formation of silicides and free carbon or formation of carbides and silicides. The latter is more likely to occur in the presence of Cr while the former occurs in the presence of Ni. The simultaneous occurrence of these two elements is expected to lead to the formation of complex reaction layers between SiC and the surrounding matrix, dominated by the Cr carbides formation according to the sequence SiC/Cr_5Si_3C/Cr_7C_3/$Cr_{23}C_6$/Cr [42].

As a matter of fact, at temperatures higher than 1000°C like the ones used during annealing, Cr carbides are the most stable carbides in the system, followed by silicon carbide. The calculated free energy of formation of Cr_7C_3 at 1000°C is of –77.21 kJ/mol, while it is –75.31kJ/mol for SiC [43]. The excess carbon deriving from decomposition of SiC can also lead to the formation of interstitial carbides, but at lower quantity than expected, as confirmed by microhardness values (Figure 9) and element maps distribution of Si and Cr in Figure 2(b).

Independently on the kind of starting powders (mixed or prealloyed), after heat treatment the same microstructure was detected: coarse equiaxic grains and coarse platelets of a second phase (Figure 5).

The microstructures due to complicated reactions of the inter-diffusion processes into the HEAs precursor after heat treatment, were observed. On the transversal sections of both kinds of samples (Figure 5) the SiC reinforcement particles completely disappeared and large platelets of a second phase have formed in their

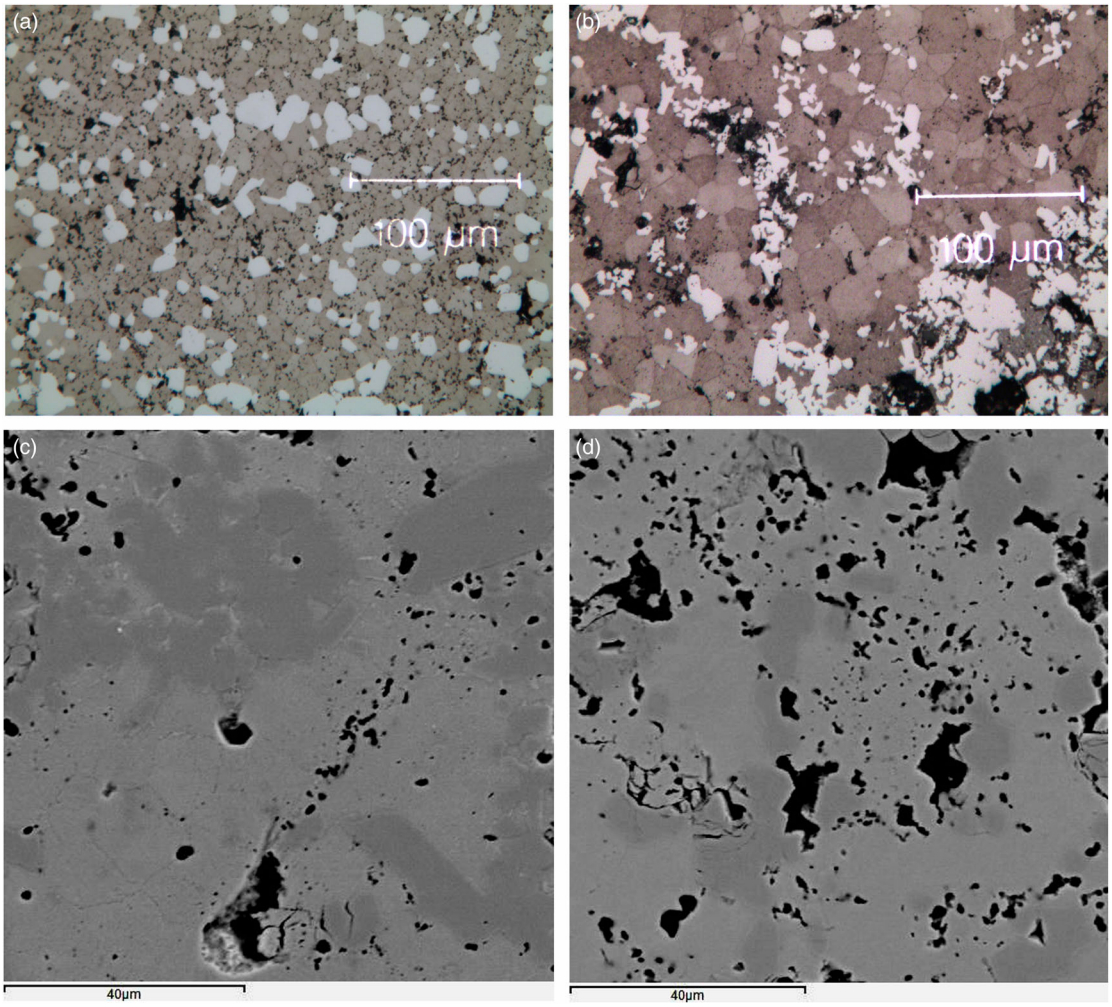

Figure 5. Microstructure of HEAs after heat treatment.

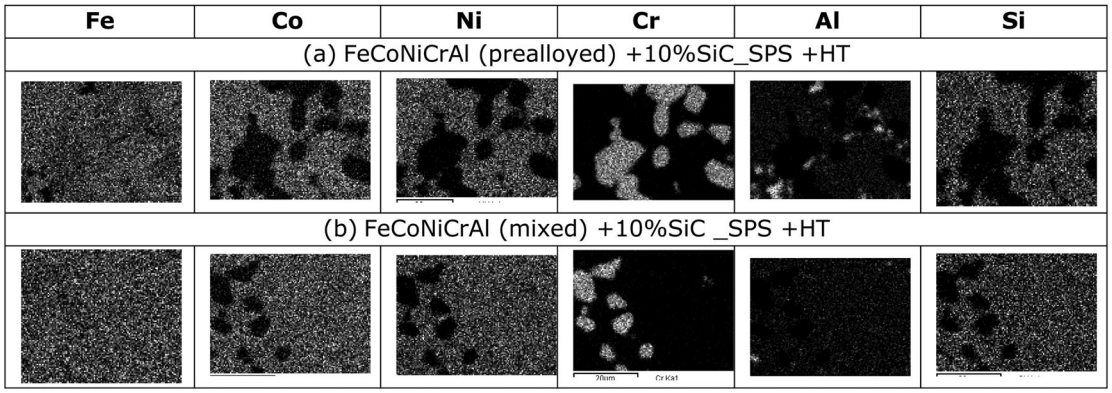

Figure 6. Element map distribution of FeCoNiCrAl + 10%SiC obtained by SPS of (a) prealloyed and (b) mixed powder.

Table 2. EDS analysis of the two zones detected: Solid Solution with fine precipitates and a Cr–Fe richer (SS-2) phase with M3C2 carbides.

	at [%]		at [%]	
Element	Cr–Fe Rich	Co–Ni–Al-rich	Cr–Fe Rich	Co–Ni–Al-rich
Fe	21.68	16.43	21.26	16.95
Co	5.94	21.75	8.12	22.27
Ni	1.12	24.58	3.49	24.46
Cr	70.34	2.11	63.90	2.25
Al	0.89	19.71	1.65	18.26
Si	0.03	15.42	1.57	15.81

place. In the case of prealloyed HEAs, the platelets of the second phase result to be more uniformly distributed. The platelets are likely to be the reaction products of the starting HEAs transition metals like Cr, Fe, Ni and Co, with SiC, leading to the formation of carbides and silicon-enriched alloys, as previously discussed [38].

To better clarify the element distribution, the EDS maps of heat-treated samples are shown in Figure 6. The samples exhibit a homogenous distribution of Si, deriving from the SiC dissociation [32], which probably acted as nucleating agent of a BCC phase, in agreement with literature [44].

Regarding HEAs systems, in agreement with literature [28,39], the EDS analyses revealed the presence of two compositionally different phases, as shown in Table 2: one solid solution named SS-2 and the other named SS-1. The former contains fine precipitates as better documented by the SEM image of Figure 7, the latter was a Cr–Fe richer phase with Cr carbides formed as the result of SiC decomposition [38].

Mechanical properties were preliminary investigated by instrumented indentation and microhardness testing on heat-treated samples. The newly formed solid solution, Si-enriched, BCC, showed completely different mechanical properties compared to the same alloy before the heat treatment.

Nano-indentation tests on the two different zones, identified by the previous analyses, are collected in Table 3. HV and E of the isomorphic samples, i.e. the two zones having different chemical composition but characterised by the crystal structure, are shown in Figure 8 and Figure 9 respectively. After annealing both values were increased thanks to the precipitation of carbide. The microhardness results (Figure 10) were compared with the ones measured in a previous work by the present authors [26], without the introduction of SiC as reinforcement: as expected, the presence of SiC leads to a higher hardness value. This high hardness can be interpreted on the basis of fine carbide precipitations and of solid solution strengthening, the latter being evident from the high hardness obtained by nano indentation of each of the two isomorphic

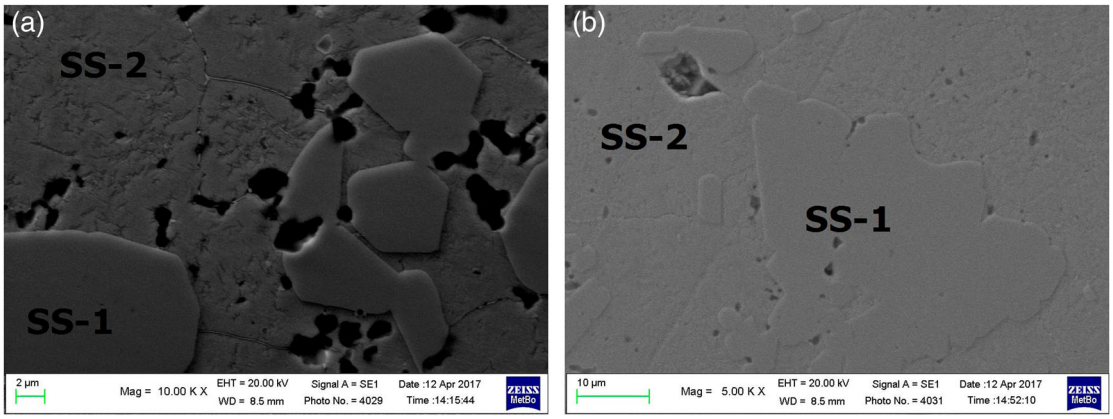

Figure 7. (a) Prealloyed and (b) mixed HEAs microstructures after heat treatment.

Table 3. Mechanical properties.

Before heat treatment					
FeCoNiCrAl (mixed) + 10%SiC_SPS					
		HIT	HV	E (GPa)	HV1
Fe–Cr-rich	Average	7099.6	1017.7	272.8	726.1 ± 22.8
	Std dev	1765.6	181.04	28.3	
Co–Ni–Al-rich	Average	11064	905.2	226.1	
	Std dev	1567.2	132.4	34.2	
FeCoNiCrAl (prealloyed) + 10%SiC_SPS					
		HIT	HV	E (GPa)	HV1
Fe–Cr-rich	Average	6911.6	662.6	223.8	810.9 ± 21.2
	Std dev	651.1	60.3	22.4	
Co–Ni–Al-rich	Average	7154.6	640.0	181.3	
	Std dev	512.2	47.4	20.1	
After heat treatment					
FeCoNiCrAl (mixed) + 10%SiC_SPS_HT					
		HIT	HV	E (GPa)	HV1
Fe–Cr-rich	Average	14994.8	1325.5	278.2	795.4 ± 22.0
	Std dev	2512.4	211.7	15.3	
Co–Ni–Al-rich	Average	9766.1	914.8	258.7	
	Std dev	298.4	27.6	10.3	
FeCoNiCrAl (prealloyed) + 10%SiC_SPS_HT					
		HIT	HV	E (GPa)	HV1
Fe–Cr-rich	Average	10681.6	1148.3	226.9	951.9 ± 25.8
	Std dev	2124.1	174.5	17.7	
Co–Ni–Al-rich	Average	11597.9	1066.9	233.2	
	Std dev	666.4	61.6	17.6	

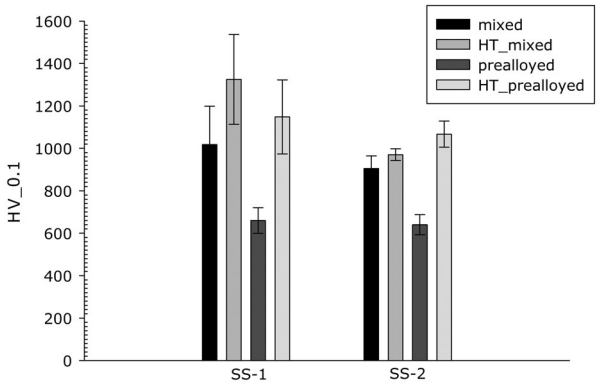

Figure 8. E [GPa] calculated in the SS-2 (Cr–Fe rich phase) and solid solution (SS-1).

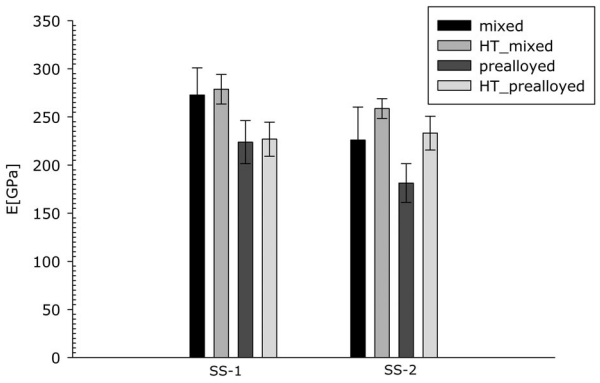

Figure 9. HV0.1 calculated in the SS-2 (Cr–Fe rich phase) and solid solution (SS-1).

phases. As well-known, precipitation hardening is designed to remarkably increase strength and toughness by the formation of extremely fine precipitates in the matrix. Following annealing of the starting

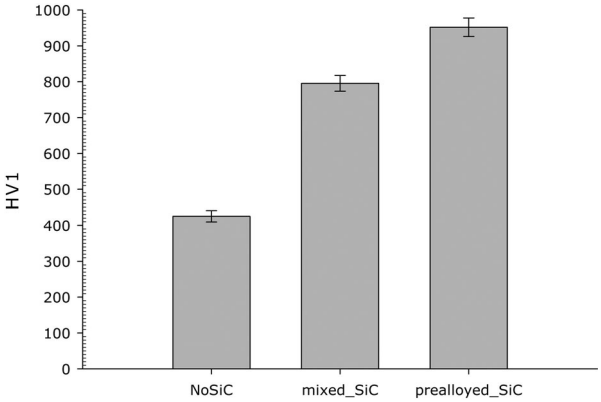

Figure 10. HV1

solid solution, the resulting matrix was supersatured with the precipitate-forming silicides which nucleated uniformly throughout the matrix, see BSE image in Figure 7.

Rather interestingly, the measured hardness values of the solid solutions in both samples are near the hardness of the carbides [45] and, despite the isomorphism of samples, as evidenced by SEM-EDS analysis, the micro hardness of the two different phases resulted similar. The hardness in case of HEA prepared starting from mixed powders resulted, prior to annealing, higher than in case of prealloyed powders. This effect might be ascribed to the different SiC reactivity demonstrated by the micrographs and temperature displacement graphs shown in Figure 3 (a–f). In both cases, as the result of SiC reactivity, the formation of reinforcing silicides and carbides is expected. However the SiC decomposition occurs to a larger extent when using mixed powders. This difference is mitigated by the high-temperature annealing, conducted above the instability temperature of SiC in presence of Fe, Ni and Cr: in this case the formation of the reinforcing precipitates occurs with SiC exposed to the same HEA matrix obtained by SPS and the resulting hardness values are similar, independently of the type of powders precursors used.

Conclusions

In this work FeCoNiCrAl HEAs reinforced with uniformly distributed SiC ceramic particles were synthesised using the powder metallurgy route. SPS was used as a reactive sintering technique due to its rapid heating and possibility to apply pressure during synthesis. The synthesis produced a single isomorphic BCC structure independently of the starting powders mixture (prealloyed or mixed). The prealloyed powders permitted to obtain a slightly more homogenous microstructure than the simply mixed one. Instead, the use of mixed powders led to a larger formation of liquid phase, which subsequently affected the SiC reinforcement and microhardness. The addition of

SiC, which is unstable at high temperatures due to the presence of transition metals, leads to modification of the original HEA matrix with Si and the precipitation of fine metal transition silicides and chromium carbide. The formation of fine carbide and silicides increases the hardness of alloys, as demonstrated by mechanical tests.

Disclosure statement

No potential conflict of interest was reported by the authors.

Notes on contributors

Elena Colombini is a postdoctoral research fellow at the Department of Engineering "Enzo Ferrari", University of Modena and Reggio Emilia. Her research activity is focussed on the synthesis of new high entropy alloys through metal powder technology. Together with her supervisor (Prof. Paolo Veronesi) she also design new microwave applicators for several employments.

Magdalena Lassinantti Gualtieri is a research fellow at the Department of Engineering "Enzo Ferrari", University of Modena and Reggio Emilia. She is specialized in synthesis and microstructural characterization of inorganic materials. Her most recent research activities involve development of sustainable building materials.

Roberto Rosa is a postdoctoral research fellow at the Department of Engineering "Enzo Ferrari", University of Modena and Reggio Emilia, and adjunct Professor of Chemistry at the Dipartimento di Scienze e Metodi per l'Ingegneria at the same University as well as at the Dipartimento di Economia Scienze e Diritto at the Università degli Studi della Repubblica di San Marino. His research activities are mainly focused on the use of microwave energy in organic and inorganic chemical synthesis, as well as in processing of materials in general.

Fabrizio Tarterini, PhD, head technician of the Metallurgy Laboratory at DIN Departement, Departement of Industrial Engineering, and expert in Spectroscopic Techniques Paolo Veronesi, Professor of Material Science at the Department of Engineering "Enzo Ferrari", University of Modena and Reggio Emilia. His research activity is mainly focussed on the thermal applications of microwaves. He is also active in the ceramic field, in particular as far as composite materials and refractory materials are concerned. During last decade he has been using commercial electromagnetic modelling software (Concerto 3.5, Comsol Multyphisics) in order to design new microwave applicators for high and low temperature heat treatments and microwave plasmas. Recently, he dedicated intensively to the development of microwaves applications to metals, high entropy alloys and intermetallics. His research activity lead to many collaborations, either National or International, mainly regarding dielectric heating and materials processing.

Mario Zadra was one of the founder of K4Sint, where he has been worked since 2007. He was graduated and received the PhD in Materials Engineering at the University of Trento with a thesis on "Effect of strain rate and sample geometry on the ductility of aluminium alloys". He is interested in all the technologies about powder metallurgy, particularly press & sint, metal injection moulding, spark plasma sintering and additive manufacturing.

Angelo Casagrande, Professor of Metallurgy at the Department of Industrial Engineering-DIN -Bologna University. His researcher is aimed to the production of innovative metal alloys, their behaviour in exercise, protective coatings and intermetallics, obtained by reactive synthesis and massive damping materials to reduce mechanical vibrations in structural components.

ORCID

E. Colombini http://orcid.org/0000-0002-0268-8027
M. Lassinantti Gualtieri http://orcid.org/0000-0001-7317-2661

References

[1] Yeh JW, et al. Nanostructured high-entropy alloys with multiple principal elements: novel alloy design concepts and outcomes. Adv Eng Mater. 2004;6(5):299–303.
[2] Cantor B, et al. Microstructural development in equiatomic multicomponent alloys. Mater Sci Eng, A. 2004;375–377:213–218.
[3] Yeh JW. Recent progress in high-entropy alloys, annales de chimie. Science des Materiaux (Paris). 2006;31(6):633–648.
[4] Liu L, et al. Effects of Sn element on microstructure and properties of SnxAl2.5FeCoNiCu multi-component alloys. J Alloys Compd. 2016;654:327–332.
[5] Tang Z, et al. Tensile ductility of an AlCoCrFeNi multi-phase high-entropy alloy through hot isostatic pressing (HIP) and homogenization. Mater Sci Eng A. 2015;647:229–240.
[6] Poletti MG, et al. Development of a new high entropy alloy for wear resistance: FeCoCrNiW0.3 and FeCoCrNiW0.3 + 5 at.% of C. Mater Des. 2017;115:247–254.
[7] Wang R, et al. Evolution of microstructure, mechanical and corrosion properties of AlCoCrFeNi high entropy alloy prepared by direct laser fabrication. J Alloys Compd. 2017;694:971–981.
[8] Senkov ON, et al. Mechanical properties of Nb25Mo25Ta25W25 and V20Nb20Mo20Ta20W20 refractory high entropy alloys. Intermetallics. 2011;19(5):698–706.
[9] Tabachnikova ED, et al. Mechanical properties of the CoCrFeNiMnVx high entropy alloys in temperature range 4.2–300 K. J Alloys Compd. 2017;698:501–509.
[10] Gludovatz B, et al. A fracture-resistant high entropy alloy for cryogenic applications. Science. 2014;345:1153–1158.
[11] Miracle DB, Senkov ON. A critical review of high entropy alloys and related concepts. Acta Mater. 2017;122:448–511.
[12] Zhang Y, et al. Microstructures and properties of high-entropy alloys. Prog. Mat. Sci. 2014;61:1–93.
[13] Joseph J. Comparative study of the microstructures and mechanical properties of direct laser fabricated and arc-melted AlxCoCrFeNi high entropy alloys. Mater Sci Eng A. 2015;633:184–193.
[14] Sriharitha R, et al. Phase formation in mechanically alloyed AlxCoCrCuFeNi (x ¼ 0.45, 1, 2.5, 5 mol) high entropy alloys. Intermetallics. 2013;32:119–126.
[15] Tariq NH, et al. Effect of W and Zr on structural, thermal and magnetic properties of AlCoCrCuFeNi high entropy alloy. J Alloys Compd. 2013;556:79–85.

[16] Hong SI, et al. Thermally activated deformation and the rate controlling mechanism in CoCrFeMnNi high entropy alloy. Mat Sci Eng A. 2017;682:569–576.
[17] Varalakshmi S, Kamaraj M, Murty BS. Processing and properties of nanocrystalline CuNiCoZnAlTi high entropy alloys by mechanical alloying. Mater Sci Eng A. 2010;527:1027–1030.
[18] Katakam S, et al. Laser assisted high entropy alloy coating on aluminum: microstructural evolution. J Appl Phys. 2014;116:104906/1-104906-6.
[19] Qiu XW, et al. Microstructure and corrosion resistance of AlCrFeCuCo high entropy alloy. J Alloys Compd. 2013;549:195–199.
[20] Ji W, et al. Mechanical alloying synthesis and spark plasma sintering consolidation of CoCrFeNiAl high entropy alloy. J Alloys Compd. 2014;589:61–66
[21] Liu Y, et al. Preparation of superfine-grained high entropy alloy by spark plasma sintering gas atomized powder. Intermetallics. 2016;68:16–22.
[22] Mohanty S, et al. Powder metallurgical processing of equiatomic AlCoCrFeNi high entropy alloy: microstructure and mechanical properties. Mat Sci Eng A. 2017;679:299–313.
[23] Soare V. Electrochemical deposition and microstructural characterization of AlCrFeMnNi and AlCrCuFeMnNi high entropy alloy. Appl Surf Sci. 2015;358:533–539.
[24] Veronesi P, et al. Microwave assisted synthesis of Si-modified Mn25FexNi25Cu(50−x) high entropy alloys. Mater Lett. 2016;162:277–280.
[25] Veronesi P, et al. Microwave processing of high entropy alloys: a powder metallurgy approach, accepted chemical engineering and processing: process intensification – In Press, Corrected Proof. [cited 2017 March 9]. Available from: https://doi.org/10.1016/j.cep.2017.02.016
[26] Colombini E, et al. High entropy alloys obtained by field assisted powder metallurgy route: SPS and microwave heating. Mater Chem Phys, Accepted. [cited 2017 July 1]. Available from: doi.org/10.1016/j.matchemphys.2017.06.065
[27] Veronesi P, et al. Microwave-Assisted preparation of high entropy alloys. Technologies. 2015;3:182–197.
[28] Zhang C, et al. Understanding phase stability of Al-Co-Cr-Fe-Ni high entropy alloy. Mater Des. 2016;109:425–433.
[29] Metaxas AC, Meredith RJ. Industrial microwave heating, IEE power engineering series 4, Published by Peter Peregrinus Ltd., 1983, Section 7.2, London: UK.
[30] Cannillo V, et al. Mechanical performance and fracture behaviour of glass-matrix composites reinforced with molybdenum particles. Compos Sci Technol. 2005;65(7–8):1276–1283.
[31] Peng Y, Miao H, Pen Z. Development of TiCN-based cermets: mechanical properties and wear mechanism. Int J Refract Met H. 2013;39:78–89.
[32] Rogal L, et al. Effect of SiC nano-particles on microstrucutre and mechanical properties of the CoCrFeMnNi high entropy alloy. J Alloys Compd. 2017;708:344–352.
[33] Penchal Reddya M, et al. Structural and mechanical properties of microwave sintered alsingle bondNi50Ti50 composites. J Sci: Adv Mater Dev. 2016;1(3):362–366.
[34] Habibur Rahman M, Mamun Al Rashed HM. Characterization of silicon carbide reinforced aluminum matrix composites. Procedia Eng. 2014;90:103–109.
[35] MCColm IJ. Ceramic science for materials technologists. London: Leonard Hill; 1983, p. 239–423.
[36] Bodukuria AK, et al. Fabrication of Al–SiC–B4C metal matrix composite by powder metallurgy technique and evaluating mechanical properties. Perspect Sci. 2016;8:428–431.
[37] Tishchenko IY, Ilchenko OO, Kuzema PO. TGA-DSC-MS analysis of silicon carbide and of its carbon-silica precursor, chemistry. Phys Technol Surf. 2015;6(2):216–223.
[38] Pan Y, Baptista JL. Chemical instability of silicon carbide in the presence of transition metals. J Ceram Soc. 1996;79(8):2017–2026.
[39] Negita K. Effective sintering aids for silicon carbide ceramics: reactivities of silicon carbide with various additives. J Am Ceram Soc 1986;69(12):C-308–C-310.
[40] Tsai K-Y, Tsai M-H, Yeh J-W. Sluggish diffusion in Co–Cr–Fe–Mn–Ni high-entropy alloys. Acta Mater. 2013;61:4887–4897.
[41] Oliver WC, Pharr GM. An improved technique for determining hardness and elastic modulus using load and displacement sensing indentation experiments. J Mater Res. 1992;7:1564–1583.
[42] Kumar A. Analysis of Si addition on phase formation in AlCoCrCuFeNiSix high entropy alloys. Mater Lett. 2017;188:73–76.
[43] Park JS, Landry K, Perepezko JH. Kinetic control of silicon carbide/metal reactions. Mater Sci Eng A. 1999;259(2):279–286.
[44] Chase MWJr., et al. JANAF thermochemical tables. J Phys Chem Ref Data. 1985;14(Suppl. 1):1881–1991
[45] Durand-Charre M. Microstructure of steels and cast irons, ed. Springer Berlin Heidelberg (2003) Appendices 22–8.